# MULTI-OBJECTIVE OPTIMIZATION OF UWB MONO-POLE ANTENNA

**S. Chamaani, M. S. Abrishamian, and S. A. Mirtaher**

Faculty of Electrical Engineering
K.N. Toosi University of Technology
P. O. Box 16315-1355, Tehran, Iran

**Abstract**—This paper presents a novel multi-objective optimization of printed microstrip-fed monopole antenna for ultra wideband (UWB) applications. Two objective functions are minimized in this design: return loss and transient distortion. Using this method, a set of optimum antennas are achieved instead of a single design. Optimization is performed to reduce distortion in different scenarios. When distortion reduction only in $E$-plane or in both of $E$- and $H$-planes is considered, the obtained set of applying this algorithm dominates reported UWB antennas. Therefore, the obtained result provides a set of proper designs for UWB systems with random physical orientationt.

## 1. INTRODUCTION

In recent years, interesting capabilities of UWB technology has provide an active research area in academic and industrial level. Among UWB elements, antennas have an important effect on signal quality. A UWB antenna must provide a good matching in ultra wide frequency band (3.1 GHz–10.6 GHz) dedicated by Federal Communication Commission (FCC) [1]. On the other hand, analog nature of every antenna may distort transmitted or received ultra short pulses. Ideally, this distortion must be eliminated in UWB antennas. In addition to matching and distortion, various criteria such as maximum allowed size, feed structure, and frequency notch capability may arise in different applications. These diverse considerations has made UWB antenna design a challenging problem.

---

Corresponding author: S. Chamaani (chamaani@eetd.kntu.ac.ir).

One powerful method proposed to handle such problems is using multi-objective optimization algorithms. These algorithms have two main advantages. The first is that in each run of algorithm instead of a single solution a class of optimum deigns (Pareto front) is achieved. So, with respect to imposed constraints a proper antenna among this class can be chosen. The second is that the resulted Pareto front could be used to study the trade-off between different objectives considered in optimization.

In this paper, multi-objective particle swarm optimization (MOPSO) is applied to design of microstrip-fed planar monopole antenna for UWB applications. Reduction of return loss and distortion are two main goals of MOPSO. Distortion minimization equals fidelity (correlation) factor maximization. Fidelity factor is calculated between the input waveform of antenna [2] and radiated electric field intensity at different points of far-field zone. According to the points region, MOPSO yields a set of optimum solutions. Finally a sample from this set is chosen and its numerical and experimental results are compared with Planar Circular Disk Monopole (PCDM) antenna [3]. The comparison results show that, in addition to preserving impedance bandwidth the resulted antenna presents better time response and lower distortion.

Although combination of return loss and fidelity factor in a simple way has ever been used to optimize UWB antennas, the use of multi-objective optimization is a novel way to study and design of UWB antennas.

The rest of this paper is structured as follows: Antenna design including the general description of antenna geometry, objective functions and optimization algorithms is discussed in Section 2. Simulation and experimental results are presented in Section 3 and the last section is devoted to conclusion.

## 2. ANTENNA DESIGN

Compact size and integration capability of planar antennas has made them a good candidate for UWB commercial applications. Microstrip-fed UWB antennas have been studied in many aspects such as impedance matching and radiation pattern [3]. Also multi-objective optimization has been used for simple conventional objectives [4]. However, multi-objective optimization has not been used for distortion reduction and matching enhancement. In this study, a version of multi-objective particle swarm optimization is used for minimization of two objectives: return loss and transient distortion. This section describes antenna geometry, objective definitions and MOPSO.
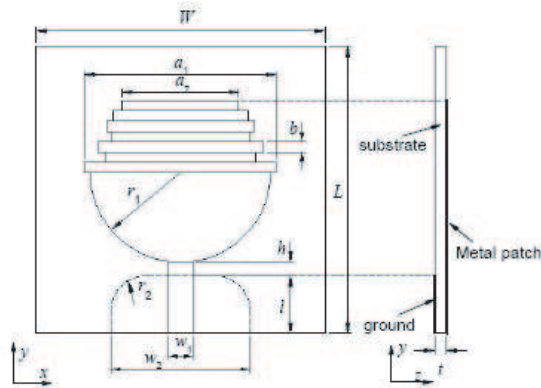
**Figure 1.** Antenna structure [4].

**Table 1.** Constant parameters (All values are given in mm).

| $r_2$ | $l$ | $w_2$ | $w_1$ | $L$ | $W$ | $t$ |
|---|---|---|---|---|---|---|
| 6.1 | 10 | 30 | 1.85 | 50 | 50 | 0.813 |

## 2.1. Antenna Geometry

The antenna structure used for optimization is shown in Fig. 1 [4]. The bottom part of radiator is a semi-disc. This semi-disc shape with proper radius leads to a low VSWR in UWB frequency band [5].

Ten variables $[a_1, \ldots, a_7, b, h, r_1]$ participate in optimization. For simplicity, $r_2$, $l$, $w_2$, $w_1$, $L$, $W$, $t$ are maintained constant during the optimization. Their values are listed in Table 1. Simulations are done for RO4003 substrate with $\varepsilon_r = 3.38$ and 0.813 thickness. The given values of Finite Ground Microstrip Line (FGMSL) [6] provide 50$\Omega$ impedance feed.

## 2.2. Optimization Objective Functions

The optimization is aimed to minimize two objective functions: return loss over the operating band and transient distortion of radiated pulses.

These objective functions are as follows:

1) The corresponding function of return loss is:

$$f_1 = \max_{f \in [3.1, 10.6\,\text{GHz}]} \{S_{11}\} \tag{1}$$

2) The corresponding function of distortion is:

$$f_2 = 1 - \left( \sum_{i=1}^{n} CF\left(\theta_i, \varphi_i\right) \right) / n \qquad (2)$$

where $CF(\theta, \varphi)$ is the normalized correlation (correlation factor) calculated between the input signal of antenna $S_{in}(t)$ and the signal detected by a virtual probe situated at the far-zone along a specified direction $S_{\theta,\varphi}(t)$. $n$ is the number of specified directions. The correlation factor is calculated as follows:

$$CF(\theta, \varphi) = \max_{\tau} \left\{ \frac{\int S_{in}(t) S_{\theta,\varphi}(t - \tau) dt}{\sqrt{\int S_{in}^2(t) dt} \sqrt{\int S_{\theta,\varphi}^2(t) dt}} \right\} \qquad (3)$$

In all simulations, the fifth derivative of Gaussian pulse is used as excitation signal. This signal is given by:

$$S_{in}(t) = GM_5(t) = \left( -\frac{t^5}{\sqrt{2\pi}\sigma^{11}} + \frac{10t^3}{\sqrt{2\pi}\sigma^9} - \frac{15t}{\sqrt{2\pi}\sigma^7} \right) \exp\left( \frac{-t^2}{2\sigma^2} \right) \qquad (4)$$

The excitation signal and its spectral density are presented in Fig. 2. With adjusting the parameters of this pulse, it complies with FCC mask limitations, properly. The appropriate value for $\sigma$ is 51 ps to satisfy the FCC mask for indoor UWB systems (Fig. 2(b)). The reminder of this section describes the algorithm applied to achieve these two goals: minimum of return loss and maximum of correlation factor in different angles.



(a)                                                (b)
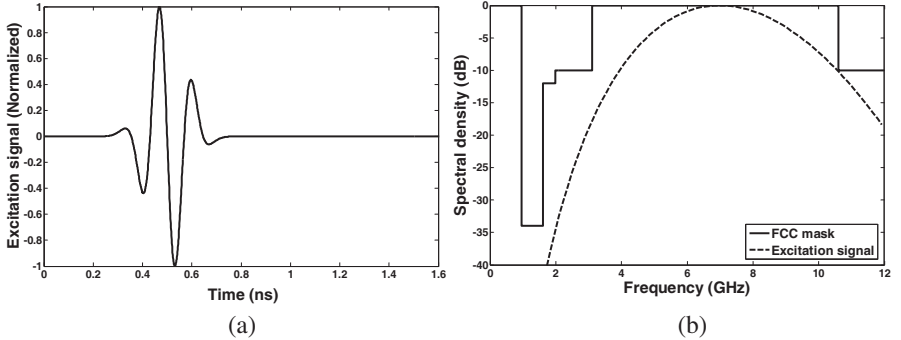
**Figure 2.** Excitation signal (a) and its spectral density (b).

## 2.3. Particle Swarm Optimization (PSO)

Recently, Particle Swarm Optimization (PSO) has been used in many engineering design problems [7–9]. PSO is a population based algorithm used to visualize the movement of a bird's flock [10]. PSO is initialized with a random population (i.e., particles) flown through a hyper dimensional search space. Each particle has an adaptable velocity and a memory remembering the best position has ever been visited by it.

In a D-dimensional search space, the $i$-th particle of the swarm is presented by a D-dimensional vector $X_i = (x_{i1}, x_{i2}, \ldots, x_{iD})^T$. Corresponding velocity of $i$-th particle is also a D-dimensional vector $V_i = (v_{i1}, v_{i2}, \ldots, v_{iD})^T$. The best experience of $i$-th particle (Pbest) is denoted as $P_i = (p_{i1}, p_{i2}, \ldots, p_{iD})^T$ . Let $g$ be the index of the best particle in the swarm and the superscripts denote the iteration number. In the global best (gbest) version of PSO, particles are updated according to the following equations:

$$v_i^{t+1}(d) = wv_i^t(d) + c_1 rand\big(p_i^t(d) - x_i^t(d)\big) + c_2 rand\big(p_g^t(d) - x_i^t(d)\big) \quad (5)$$
$$x_i^{t+1}(d) = x_i^t(d) + v_i^{t+1}(d) \quad (6)$$

where $v_i^t(d)$ and $x_i^t(d)$ represent the current velocity and the position of the $d$-th dimension of the $i$-th particle respectively and $rand$ is a uniform random number in the range [0, 1]; $c_1$, $c_2$ are called acceleration constants and selected to be 2.05 and $w$ is the inertia weight. The inertia weight linearly decreases from 0.9 at the beginning of the optimization to o.4 towards the end [11, 12].

Above equations represent basic form of single objective PSO. In the next subsection, basics of multi-objective optimization is expressed.

## 2.4. Multi-Objective PSO (MOPSO)

The main purpose of every multi-objective algorithm is to find the Pareto optimal set. To define Pareto optimal set the "domination" concept must be defined as follows:

A variable $x_1$ dominates a variable $x_2$, if and only if

$$\begin{aligned} f_k(x_1) \leq f_k(x_2), \ \ \forall k = 1, \ldots, n_k \\ f_k(x_1) < f_k(x_2), \ \ \exists k = 1, \ldots, n_k \end{aligned} \quad (7)$$

A variable $x^* \in F$ is Pareto optimal if a variable $x \neq x^* \in F$ does not exist that dominates it. The set of all Pareto-optimal variables form the Pareto optimal set and the corresponding objective vectors are called Pareto front. In this problem, $n_k = 2$.

Among several existing multi-objective algorithms, MOPSO proposed by Coello Coello et al. is selected due to its ability to achieve a diverse Pareto front [13].

In this algorithm, the best non-dominated solutions have ever been visited are stored in a memory space calling archive. The position updating equation has the same form as single objective PSO. The velocity updating equation is as follows:

$$v_i^{t+1}(d) = wv_i^t(d) + c_1 rand\big(p_i^t(d) - x_i^t(d)\big) + c_2 rand\big(archive_h^t(d) - x_i^t(d)\big)$$
(8)

The term $archive_h^t$ is taken from archive. The index $h$ is selected using the algorithm proposed in [13]. In updating archive, it must remain always dominance free. The size of archive is finite. When the archive reaches to its maximum allowable capacity, those particles located in less populated areas of objective space are given priority over those lying in highly populated regions.

In addition to standard test functions (ZDT family) [14], this algorithm has been used in electromagnetic absorber design and has shown a better performance in comparison with Non-dominated Sorting Genetic Algorithm II (NSGAII) [15, 16].

## 3. NUMERICAL AND EXPERIMENTAL RESULTS

MOPSO is applied to achieve Pareto front of antenna shown in Fig. 1 for good matching and good fidelity in three different cases.

1) Case1- Fidelity is considered only in $E$-plane ($\varphi = 90°$). Three virtual probes are used in evaluation of $f_2$ ($n = 3$) [17]. These probes are situated at points $\theta_1 = 0°$, $\theta_2 = 30°$, $\theta_3 = 60°$, $\varphi_1 = \varphi_2 = \varphi_3 = 90°$.

2) Case2- Fidelity is considered only in $H$-plane ($\varphi = 0°$). Three virtual probes are used in evaluation of $f_2$ ($n = 3$). These probes are located at points $\theta_1 = 30°$, $\theta_2 = 60°$, $\theta_3 = 90°$, $\varphi_1 = \varphi_2 = \varphi_3 = 0°$.

3) Case3- Fidelity is calculated for both of $E$- and $H$-planes. Six virtual probes are used in evaluation of $f_2$ ($n = 6$). These probes are located at points
$\theta_1 = 0°, \theta_2 = 30°, \theta_3 = 60°, \varphi_1 = \varphi_2 = \varphi_3 = 90°$
$\theta_4 = 30°, \theta_5 = 60°, \theta_6 = 90°, \varphi_4 = \varphi_5 = \varphi_6 = 0°$ .

The parameters of MOPSO are listed in Table 2.
The resulted Pareto fronts are illustrated in Figs. 3–5, respectively.
In Fig. 3, after 1000 function evaluations (population size × maximum generation) a set of 19 optimum design has been achieved. With

respect to relative importance of $f_1$ or $f_2$, any design from Pareto optimal set could be chosen. Usually $\max_{f \in [3.1, 10.6\,\text{GHz}]} \{S_{11}\} < -10\,\text{dB}$ is a necessary condition in practice. Fig. 3 shows that 12 designs which are below the dashed line satisfy this condition.

The antenna denoted by Design1 is selected as a case study. In the rest of this section frequency and time domain characteristics of Design1 (optimized) antenna is investigated and compared with PCDM antenna (Fig. 6). Optimized antenna structure is shown in Fig. 7 and its corresponding dimensions are listed in Table 3.
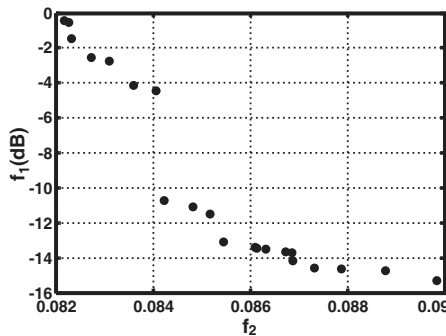
**Table 2.** Parameters of MOPSO.

| Population size | 10 |
|---|---|
| Maximum generation | 100 |
| Maximum archive size | 100 |
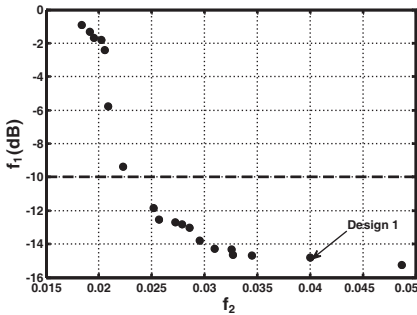


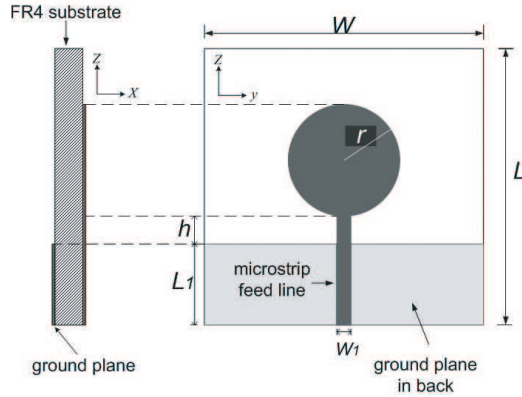**Figure 3.** Resulted Pareto front of case1.
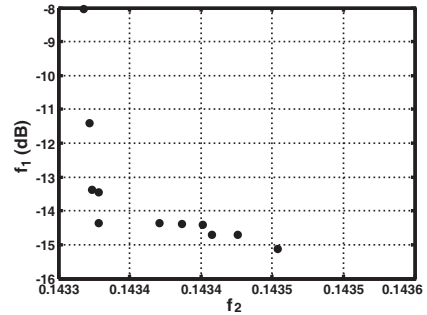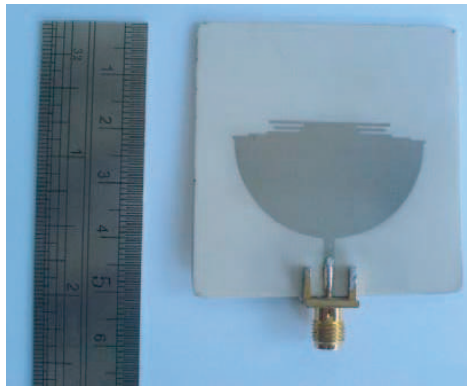


**Figure 4.** Resulted Pareto front of case2.



**Figure 5.** Resulted Pareto front of case3.

**Table 3.** Optimized antenna dimensions.

| $w_1$ | $w_2$ | $l$ | $b$ | $h$ | $r_1$ | $r_2$ |
|-------|-------|------|------|------|-------|-------|
| 1.85  | 30    | 10   | 0.5  | 0.5  | 17.7  | 6.1   |
| $a_1$ | $a_2$ | $a_3$ | $a_4$ | $a_5$ | $a_6$ | $a_7$ |
| 36.2  | 30.5  | 23.3 | 11   | 21   | 9.6   | 22.8  |



**Figure 6.** Structure of PCDM antenna [3].



**Figure 7.** Structure of optimized antenna.

Simulated and measured values of $|S_{11}|$ are shown in Fig. 8. The electrical parameters have been measured by using a HP8410C network analyzer. As it can be observed, the fabricated Design1 antenna presents a good matching in 3.6–11 GHz frequency band.

Since virtual probes are located in the $E$-plane ($\varphi = 90°$), we expect the Tx/Rx system frequency domain transfer function in face to face scenario to become more flat. This transfer function is plotted for optimized and PCDM antennas. Fig. 9. and Fig. 10 illustrate that variations of $|S_{21}|$ and group delay are reduced noticeably for the optimized antenna.

Maximum variation of $|S_{21}|$ for optimized and PCDM antennas are 22 dB and 30 dB respectively. Also, maximum fluctuation of group delay for the optimized antenna is 0.35 ns whereas the corresponding value for PCDM antenna is 1.4 ns. The measurement setup for $|S_{21}|$, consists of two identical antennas that are placed 30 cm apart and parallel to each other in a non-controlled environment. As shown in Fig. 11 the measured value of $|S_{21}|$ reasonably agrees with the simulated one.

$E$-plane CF pattern is plotted in Fig. 12. As it is shown, the CF has been improved in almost all directions (usually off-boresight
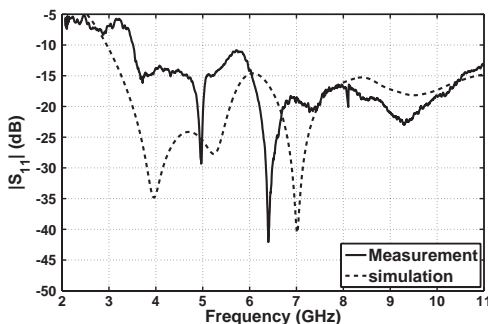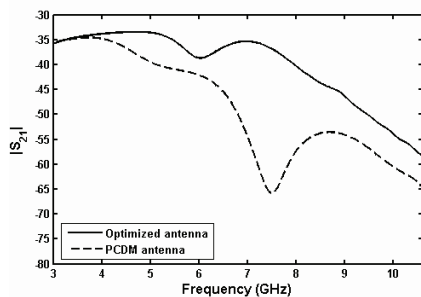
**Figure 8.** Return loss of Design1 antenna.

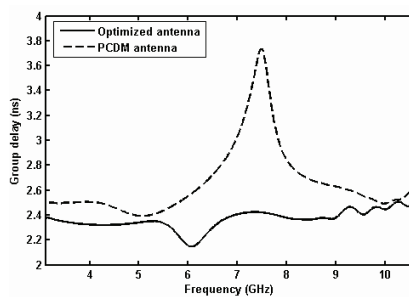**Figure 9.** Simulated value of $|S_{21}|$ in face to face scenario.
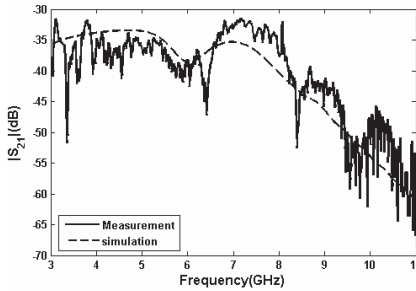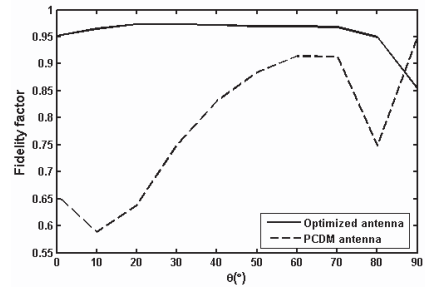
**Figure 10.** Simulated group delay in face to face scenario.

**Figure 11.** Measurement result of $|S_{21}|$ in face to face scenario.

**Figure 12.** Fidelity factor in $E$-plane ($\varphi = 90°$).

directions-near $\theta = 90°$-does not have practical importance). The higher value of CF indicates that optimized antenna is a low distortion component and can improve the signal quality extremely.

These simulation and experimental results show the primacy of Design1 in many frequency and time domain aspects. However, Design1 is a typical sample from Pareto front. For example, 12 antennas with acceptable matching and lower dispersion can be selected from resulted Pareto.

The case1 considers fidelity only in $E$-plane. Symmetric nature of $E$-plane leads to high values for fidelity in it. Therefore, fidelity in asymmetrical $H$-plane is also considered in case2 and case3. Fig. 4 shows that fidelity values are very low in case2. In other words, the signals are more degraded in $H$-plane. For PCDM antenna, $f_2 = 0.11$ which means circular shape, leads to higher fidelity in $H$-plane.

In case3, which considers both of $E$- and $H$-planes, $f_2$ values are less than 0.09. In this case, $f_2 = 0.17$ for PCDM antenna. For circular $E$-monopole which is recently introduced [19], $f_2 = 0.093$.

This antenna is designed for using in unpredictable orientations. Therefore, case3 as a rough estimation of random placement of antennas has the most practical importance and the method proposed in this paper yields a set of optimized antennas which have the best performance in this scenario.

## 4. CONCLUSION

Multi-objective Particle Swarm Optimization has been applied to design of UWB microstrip-fed planar monopole antenna. Two distinct objectives were considered in this optimization are good matching and low distortion. MOPSO yields a set of optimum designs in a single run.

A sample antenna from achieved Pareto front was studied in frequency and time domain aspects. Time domain simulation results show that $E$-plane fidelity factor of optimized antenna has been enhanced greatly in comparison with antennas reported in literature.

Optimization has been performed to reduce distortion in different scenarios. Although circular shape for radiator presents better fidelity in $H$-plane, in $E$-plane or in both of $E$- and $H$-planes the resulted set from MOPSO dominates reported circular UWB antennas.

## REFERENCES

1. FCC Report and Order for Part 15 Acceptance of Ultra Wideband (UWB) Systems from 3.1–10.6 GHz, FCC, Washington, DC, 2002.

2. Sheng, H., P. Orlik, A. M. Haimovich, L. J. Cimini, and J. Zhang, "On the spectral and power requirements for Ultra-Wideband transmission," *Proc. IEEE Int. Conf. Commun. (ICC)*, 738–742, 2003.

3. Liang, J., L. Guo, C. C. Chiau, X. Chen, and C. G. Parini, "Study of a printed circular disc monopole antenna for UWB systems," *IEEE Transactions on Antennas and Propagation*, Vol. 53, No. 11, Nov. 2005.

4. Yang, X. S., K. F. Man, S. H. Yeung, J. L. Li, and B. Z. Wang, "Ultrawideband planar antenna optimized by a multi-objective evolutionary algorithm," *Proc. IEEE Asia-Pacific Microwave Conference*, 649–652, Dec. 2007.

5. Kerkhoff, A. J., R. L. Rogers, and H. Ling, "Design and analysis of planar monopole antennas using a genetic algorithm approach," *IEEE Transactions on Antennas and Propagation*, Vol. 52, No. 10, 2079–2718, Oct. 2004.

6. Sun, S. and L. Zhu, "Unified equivalent circuit model of finite-ground microstrip line open-end discontinuities using MoM-SOC technique," *IEICE Trans. Electron.*, Vol. E87-C, No. 5, 828–831, May 2004.

7. Chamaani, S., S. A. Mirtaheri, and M. Aliyari, "Design of very thin wide band absorbers using particle swarm optimization," *Proc. 12th International Symposium on Antenna and Applied Electromagnetic [ANTEM] and Canadian Radio Sciences [URSI/CNC]*, 629–632, 2006.

8. Chamaani, S., S. A. Mirtaheri, and M. Aliyari, " Design of very thin wide band absorbers using modified local best particle swarm optimization," *Int. J. Electron. Commun. (AEÜ)*, Vol. 62, 549–556, 2008.

9. Chamaani, S. and S. A. Mirtaheri, "Planar UWB monopole antenna optimization to enhance time-domain characteristics using PSO," *Proc. International Symposium on Antenna and Propagation (ISAP 08)*, 553–556, Taipei, Taiwan, 2008.

10. Kennedy, J. and R. Eberhart, "Particle swarm optimization," *Proc. IEEE International Conference on Neural Network*, 1942–1948, Piacataway, NJ, 1995.

11. Clerc, M. and J. Kennedy, "The particle swarm-explosion, stability, and convergence in multidimensional complex search space," *IEEE Trans. Evolutionary Computattion*, Vol. 6, No. 1, 58–73, 2002.

12. Shi, Y. and R. C. Eberhart, "Empirical study of particle swarm optimization," *Proc. Congress of Evolutionary Computation (CEC99)*, Vol. 3, 1945–1950, 1999.

13. Coello, C. A. C., G. T. Pulido, and M. S. Lechuga, "Handling multiple objectives with particle swarm optimization," *IEEE Trans. Evolutionary Computattion*, Vol. 8, 256–279, 2004.

14. Farina, M., K. Deb, and P. Amato, "Dynamic multiobjective optimization problems: Test cases, approximation, and applications," *Proc. Evolutionary Multi-Criterion Optimization*, 311–326, 2003.

15. Goudos, S. and J. N. Sahalos, "Microwave absorber optimal design using multi-objective particle swarm optimization," *Microwave and Optical Technology Letters*, Vol. 48, No. 8, 1553–1558, 2006.

16. Chamaani, S., S. A. Mirtaheri, M. Teshnehlab, M. Aliyari, and V. Seydi, "Modified multi-objective particle swarm optimization for electromagnetic absorber design," *Progress In Electromagnetics Research*, PIER 79, 353–366, 2008.

17. Telzhensky, N. and Y. Leviatan, "Novel method of UWB antenna optimization for specified input signal forms by means of genetic algorithm," *IEEE Transactions on Antennas and Propagation*, Vol. 54, No. 8, 2216–2225, 2006.

18. Telzhensky, N. and Y. Leviatan, "Planar differential elliptical UWB antenna optimization", *IEEE Transactions on Antennas and Propagation*, Vol. 54, No. 11, 3400–3406, 2006.

19. Abbosh, A. M. and M. E. Bialkowski, "Design of ultrawideband planar monopole antennas of circular and elliptical shape," *IEEE Transactions on Antennas and Propagation*, Vol. 56, No. 1, 17–23, 2006.